

¹ **A quiet-time empirical model of equatorial plasma**
² **drift in the Peruvian sector**

P. Alken

³ Department of Physics, University of Colorado, Boulder, Colorado, USA,

⁴ National Geophysical Data Center, NOAA, Boulder, Colorado, USA

P. Alken, National Geophysical Data Center, NOAA E/GC1, 325 Broadway, Boulder, CO
80305-3328, USA. (patrick.alken@noaa.gov)

5 **Abstract.** Equatorial vertical plasma drift is an important consequence
6 of the E and F region dynamos. Understanding the climatology of vertical
7 drift can provide significant insight into ionospheric phenomena, such as the
8 equatorial ionospheric anomaly. In this study we present the first empirical
9 model of vertical plasma drifts observed by the JULIA (Jicamarca Unattended
10 Long-term studies of the Ionosphere and Atmosphere) coherent scatter radar
11 located in Peru. The model, called JVDM (JULIA Vertical Drift Model), de-
12 scribes the local time, seasonal and solar flux behavior of the equatorial ver-
13 tical drifts in the Peruvian sector. The model is valid from 0800 through 1600
14 local time, which is typically when JULIA makes vertical drift measurements.
15 During very high solar flux conditions however, the model is unreliable be-
16 fore 1000 local time, due to a lack of JULIA data. The model includes a cli-
17 matology of the equatorial vertical drifts, as well as an estimate of the day-
18 to-day variability, which can be significant. The day-time drifts typically peak
19 between 1000 and 1200 LT and have amplitudes of 25-30 m/s \pm 10 m/s. The
20 model has been validated against the global empirical model of Scherliess
21 and Fejer, with a total rms difference of under 4 m/s for 1000 to 1600 LT.
22 This model will allow researchers to study daily variations in the equatorial
23 electric field by subtracting the climatological mean. Model coefficients and
24 software are available online at <http://geomag.org/models> and <http://www.earthref.org>.

1. Introduction

Equatorial vertical plasma drifts are driven by complex dynamo processes in the ionospheric E and F regions. Neutral winds on the day-side cause positive and negative charges to accumulate at the dawn and dusk terminators respectively, giving rise to the equatorial electric field (EEF) [Heelis, 2004]. This field is eastward on the day-side and westward on the night-side. The EEF in combination with the earth's magnetic field drives ion drifts which are typically upward and westward during the day-time and downward and eastward at night.

Accurately measuring and predicting vertical plasma drifts is important for the study of many physical processes in the low latitude ionosphere, including the Equatorial Ionization Anomaly (EIA) [Appleton, 1954], upper F region electron density structures [Su et al., 1995], the equatorial electrojet (EEJ) [Forbes, 1981; Alken and Maus, 2007] as well as the forecasting of low latitude ionospheric weather. There have been previous studies to model quiet-time vertical plasma drifts using observatory data as well as satellite data. Scherliess and Fejer [1999] combined measurements from the Jicamarca incoherent scatter radar (ISR) with observations from the Atmospheric Explorer E (AE-E) satellite to produce a quiet-time empirical vertical drift model at all longitudes, seasons, local time and solar flux values. Fejer et al. [2008] produced a quiet-time empirical drift model of observations from the ROCSAT-1 satellite with global longitudinal coverage. There have also been other regional empirical drift models developed [Abdu et al., 1995; Sastri, 1996; Batista et al., 1996].

45 The Jicamarca Radio Observatory (JRO) (11.95°S, 76.87°W) near Lima, Peru has been
46 measuring equatorial vertical plasma drifts at 150 km altitude since 1996 using the JULIA
47 radar. JULIA is a coherent scatter radar which makes high-quality observations of Doppler
48 150-km echoes which have been shown to yield good estimates of F region vertical ion
49 drifts [*Kudeki and Fawcett, 1993; Woodman and Villanueva, 1995*]. JULIA measures 150-
50 km vertical drifts during day-time hours at 5 minute intervals. JULIA data has enabled
51 the study of many important ionospheric processes and is especially useful due to its
52 near-continuous day-time observations of vertical drifts since 1996. However, there has
53 never been an empirical model created for the JULIA data. The model of *Scherliess*
54 *and Fejer* [1999] used the incoherent scatter radar at Jicamarca which normally operates
55 in campaign mode and does not have continuous measurements at all local times and
56 seasons. In this work we present the first empirical vertical drift model based on the
57 JULIA coherent scatter radar. This model is of interest for studies of electrodynamic
58 effects of atmospheric tides. It also provides the climatology of the equatorial plasma
59 fountain, which is the source of the equatorial ionization anomaly. Last but not least, the
60 model allows users of JULIA data to subtract the climatological mean in order to study
61 daily variations in the eastward electric field.

2. Climatological Mean Model Description

62 This empirical vertical plasma drift model was derived from JULIA coherent scatter
63 radar data in the period of August 2001 through July 2008. Only quiet-time data (K_p
64 ≤ 3) were used, in the local time sector of 0800 to 1600 when JULIA data are typically
65 available. Figure 1 shows the distribution of data over season, local time, and solar flux

66 level. There is a lack of data in the early morning (0800-1000 LT) during high solar flux
 67 at all seasons and also during June and December solstice at lower solar flux levels.

The data selection yields a total of 46,669 drift measurements. Each drift measurement is provided with an error estimate, enabling a weighted least squares fit. The model is a function of local time, season and solar activity. We use the EUVAC flux index [Richards *et al.*, 1994] for the solar activity dependence which is defined as $P = (F10.7 + F10.7A)/2$ where $F10.7A$ is the 81 day average of F10.7. The functional form of the model is given by

$$v(t, s, p) = \sum_{i=1}^{N_t} \sum_{j=1}^{N_s} \sum_{k=1}^2 a_{ijk} B_i(t) f_j(s) p^{k-1} \quad (1)$$

68 where t is local time, s is season (day of year), and p is the EUVAC solar flux proxy
 69 defined above. The coefficients a_{ijk} are to be determined and the basis functions are given
 70 by

$B_i(t)$ = i th cubic B-spline with uniform knots from

$$8 \text{ to } 16 \text{ LT} \quad (2)$$

$$f_j(s) = \begin{cases} \cos\left(\frac{(j-1)\pi s}{365.25}\right) & j \text{ odd} \\ \sin\left(\frac{j\pi s}{365.25}\right) & j \text{ even} \end{cases} \quad (3)$$

71 B-splines [De Boor, 2001] were chosen for the local time dependence since there does
 72 not appear to be a more physically natural basis available. The model of Scherliess and
 73 Fejer [1999] accounted for seasonal variation by essentially binning their data into broad
 74 seasonal bins and performing separate fits for each season. The seasonal structure of the
 75 vertical drifts is complex and not fully understood, but does have a periodic structure,
 76 most easily observed with peaks during equinox and minima during solstice [Alken and
 77 Maus, 2007; Fejer *et al.*, 2008]. The oscillatory seasonal basis functions were chosen due

78 to this observed periodicity. A linear fit was performed in the solar flux variable due to
79 the known correlation between the vertical plasma drift and solar activity.

The values of N_t and N_s were chosen by examining how the residual mean square changes as a function of these parameters. The residual mean square is defined as

$$s^2 = \frac{1}{n-p} \sum_{i=1}^n w_i [v_i - v(t_i, s_i, p_i)]^2 \quad (4)$$

80 where n is the total number of drift measurements and p is the number of parameters in
81 the model ($p = 2N_t N_s$). The weights are $w_i = 1/(\sigma_i^2 + 1)$ with units of $(m/s)^{-2}$ and the
82 values σ_i are the given error estimates with the JULIA data (in m/s). The additive factor
83 of 1 $(m/s)^2$ in the denominator ensures numerically reasonable weights when σ_i is small.
84 The v_i are the JULIA drift observations and $v(t_i, s_i, p_i)$ is the corresponding model value.
85 As more basis functions are added to the model, eventually causing over-fitting to the
86 data, s^2 will approach the true value of the error variance σ^2 [Draper and Smith, 1981].

87 Figure 2 shows the residual mean square s^2 as a function of N_t and N_s individually while
88 holding the other value constant. In both plots the residual mean square decreases as the
89 number of basis functions increases. This is most evident in the N_s plot where s^2 decreases
90 sharply as N_s increases. The N_t plot does not contain such a sharp decrease, however we
91 do see the typical asymptotic behavior as over-fitting takes place and s^2 approaches
92 the true variance σ^2 . The N_s plot does not approach an asymptotic value of s^2 within a
93 reasonable choice of N_s , which is most likely due to the high degree of variability in the
94 seasonal structure of the data. We therefore choose $N_s = 11$ which should adequately
95 describe the seasonal changes of the JULIA vertical drift data. This choice represents
96 sinusoidal basis functions up to degree 5 in the model, which will satisfactorily capture

97 the peaks during equinox and minima during solstice, as well as allow for differences
98 between March and September equinox and other smaller seasonal structures.

From the N_t figure alone, it is difficult to pinpoint the ideal value of the N_t parameter, and so we computed the Mallows C_p statistic [Draper and Smith, 1981] for each of a set of possible N_t values. The Mallows C_p is defined as

$$C_p = RSS_p/\sigma^2 - (n - 2p) \quad (5)$$

99 where RSS_p is the residual sum of squares for a model with p parameters, σ^2 is the best
100 estimate of the actual error variance, and n is the number of data points. For an accurate
101 model, C_p has an expected value of approximately p . We estimated the error variance
102 as $\sigma^2 = 34.2$ using the data in Figure 2 for $N_s = 11$ and computed the C_p statistic for
103 several possible values of N_t . A plot of C_p vs p is given in Figure 3. Any model with a
104 C_p value close to p passes the C_p test, and we see from the figure that the models with
105 $N_t \geq 7, N_s = 11$ lie on the line $C_p = p$. However the model with $N_t = 7$ was chosen to
106 attempt to keep higher frequency artifacts in the local time dependence of the model to
107 a minimum. This model has 154 parameters and a C_p of 138.3. The discrepancy between
108 these two numbers is largely a result of the accuracy of the estimate of σ^2 .

109 Once suitable values of N_t and N_s were selected for the model in Eq. 1, a weighted least
110 squares regression was performed to minimize the residual sum of squares $RSS = s^2(n-p)$.
111 The calculated value of the coefficient of determination is $R^2 = 0.32$, indicating that the
112 climatological model accounts for 32% of the variation about the mean in the data. This
113 low figure clearly indicates the high degree of day-to-day variability in the equatorial
114 vertical drifts.

115 Figure 5 shows, as a function of local time and season, the vertical drift values produced
116 by the model as compared with the raw JULIA data and the Scherliess and Fejer model.
117 The JULIA data plot in the middle was created by binning the dataset into half-hour
118 bins in local time and 20 day bins in season, computing the mean of each bin, and then
119 fitting a surface using a continuous curvature gridding algorithm [*Wessel and Smith,*
120 1991] with a grid spacing of 0.3 hours in local time and 5 days in season. We see a
121 very good agreement between the model and data. All major features of the vertical
122 plasma drifts have been reproduced. The drift maxima during March and September
123 equinox and minima during June and December solstice agree well. We also see that the
124 local time behavior is well reproduced, with maxima near 1030-1130 LT. An important
125 improvement in the JVDM model compared to the Scherliess and Fejer model is the
126 allowance of differences between March and September equinox. The model of Scherliess
127 and Fejer treated both equinoxes as identical but the JULIA data indicates slightly higher
128 drift velocities during September and some asymmetries between the equinoxes at later
129 local times. These seasonal differences are illustrated in Figure 4 which clearly indicates
130 that the seasonal dependence of the Scherliess and Fejer model is insufficient to fully
131 capture the JULIA seasonal drift structure. The JVDM seasonal basis functions allow for
132 more accurate modeling of these features.

We examined the weighted residuals

$$r_i = \sqrt{w_i}(v_i - v(t_i, s_i, p_i)) \quad (6)$$

133 and do not find any systematic trend which would indicate an insufficient number of terms
134 in the model. There are a few outliers in the residuals which indicate data points that are
135 not typical of the majority of the data. These could be due to errors in those observations

136 or unusual ionospheric conditions when the measurement was made. Since it is difficult
137 to determine the exact cause of these outliers, we choose not to reject them out of hand
138 in the analysis. The weighted mean of all residuals is 1.0×10^{-13} .

3. Model Validation

139 To validate the JULIA vertical drift model (JVDM), we compared it with the empirical
140 quiet-time vertical drift model of *Scherliess and Fejer* [1999]. This model was based on
141 equatorial vertical drift data from the incoherent scatter radar (ISR) at Jicamarca as well
142 as observations from the Atmospheric Explorer E satellite. The model used Jicamarca ISR
143 data averaged from about 300 to 400 km altitude. Although JULIA makes measurements
144 at 150 km altitude, the comparison is meaningful since it has been found that vertical
145 drift velocity gradients are small. *Pingree and Fejer* [1987] analyzed Jicamarca ISR data
146 and found only small gradients within $|0.05| \text{ m s}^{-1} \text{ km}^{-1}$. *Fejer et al.* [1995] also did not
147 find significant gradients at F region altitudes using the AE-E satellite database.

When computing the rms difference between the two models, defined as

$$\epsilon = \sqrt{\frac{1}{V} \int [v(t, s, p) - v_{SF}(t, s, p)]^2 dt ds dp} \quad (7)$$

148 where the integral is taken over local times 0800 to 1600, all seasons and all solar flux
149 conditions, the result is 4.3 m/s. In the above expression, v_{SF} is the vertical drift model of
150 *Scherliess and Fejer* [1999] and v is the JULIA vertical drift model. V is the total volume
151 of parameter space. The primary contribution to this rms difference is most likely the lack
152 of JULIA data before 1000 local time, as well as the different seasonal dependence of the
153 two models. Recomputing the rms difference for the local time sector 1000 to 1600 yields
154 a value of 3.8 m/s. Computing the rms difference for 0800 to 1600 local time, but only up

155 to a maximum EUVAC index of 150 yields a value of 3.4 m/s. As mentioned above, the
156 seasonal dependence of the two models was treated differently which is also contributing
157 error, however these values are fairly reasonable and lead us to conclude this is a positive
158 validation of JVDM with the understanding that there are inaccuracies at high solar flux
159 conditions (> 150) before 10 am local time.

4. Deviation Model

Since the equatorial vertical plasma drifts are highly variable from day-to-day, the climatological mean by itself is not sufficient to describe them. We would therefore like an estimate of the standard deviation from the climatological mean. Since each measurement is taken at a specific local time, season and solar flux and is the only measurement for those particular parameters, the only variability estimate available is the absolute deviation from the mean

$$D_i = |v_i - v(t, s, p)|, \quad (8)$$

which is not the same as the standard deviation. However, if the data is normally distributed, it can be shown that the absolute mean deviation is related to the standard deviation by a constant:

$$D = \sqrt{\frac{2}{\pi}} \sigma. \quad (9)$$

Therefore we present a model of the day-to-day absolute deviation of the vertical drifts from their climatological mean. This model is then used to show that the vertical drifts are in fact normally distributed, so that the standard deviation can be estimated. The

same functional form was used as for the mean model:

$$D(t, s, p) = \sum_{i=1}^{N_t} \sum_{j=1}^{N_s} \sum_{k=1}^2 b_{ijk} B_i(t) f_j(s) p^{k-1} \quad (10)$$

with the same basis functions for each parameter. We performed a similar analysis to that shown in Figure 2 and found the same values of N_t and N_s were suitable as for the mean fit. We then performed an unweighted least squares fit to the model in Eq. 10. In order to show that this model is meaningful, we computed “normalized drifts”:

$$\bar{v}_i = \frac{v_i - v(t, s, p)}{\sigma(t, s, p)} = \frac{v_i - v(t, s, p)}{\sqrt{\frac{\pi}{2}} D(t, s, p)} \quad (11)$$

160 which, if the mean and deviation models are correct, will produce a dataset normally
 161 distributed with zero mean and unit standard deviation. Indeed, the mean of the \bar{v}_i
 162 dataset is 0.057 and its standard deviation is 1.006. To show that the \bar{v}_i are normally
 163 distributed, we computed a quantile-quantile plot in Figure 6a which has normal quantiles
 164 on the horizontal axis with the \bar{v}_i quantiles on the vertical axis. Since most of these lie
 165 on the line $y = x$ the normalized drift dataset is almost surely normally distributed, since
 166 other distributions would result in a deviation from this line. This indicates that our
 167 relation between the standard deviation and absolute mean deviation models is correct.
 168 This is further illustrated in Figure 6b which shows the probability density profile of the
 169 \bar{v}_i dataset along with an ideal normal distribution with zero mean and unit deviation.
 170 There is a very good agreement between the two probability functions. Figure 6c shows
 171 an example local time profile along with its \pm standard deviation curves to illustrate the
 172 high day-to-day variability of the vertical plasma drifts from their climatological mean.

5. Conclusion

173 We have presented the first empirical model of vertical plasma drifts measured from
174 150-km JULIA radar echoes. The model includes two components, one for the climato-
175 logical mean as a function of local time, season and solar activity, and one which provides
176 an estimate of the day-to-day variability of the drifts, as a function of the same param-
177 eters. The model has been validated against the global empirical model of *Scherliess*
178 *and Fejer* [1999] with good agreement. This model also incorporates for the first time
179 the complicated seasonal structure of the drifts, especially the differences between March
180 and September equinox which are not represented in the model of Scherliess and Fejer.
181 Model coefficients and software are available online at <http://geomag.org/models> and
182 <http://www.earthref.org>.

Acknowledgments

183 The Jicamarca Radio Observatory is gratefully acknowledged for providing the JULIA
184 vertical drift data. The author thanks S. Maus and C. Manoj for their helpful comments
185 on an earlier version of this manuscript.

References

- 186 Abdu, M. A., I. S. Batista, G. O. Walker, J. H. A. Sobral, N. B. Trivedi, and E. R.
187 de Paula (1995), Equatorial ionospheric electric fields during magnetospheric distur-
188 bances: Local/longitude dependencies from recent EITS campaigns, *J. Atmos. Terres.*
189 *Phys.*, *57*, 1065–83.
- 190 Alken, P., and S. Maus (2007), Spatio-temporal characterization of the equatorial elec-
191 trojet from CHAMP, Ørsted, and SAC-C satellite magnetic measurements, *J. Geophys.*

193 Appleton, E. V. (1954), The anomolous equatorial belt in the F2-layer, *J. Atmos. Terres.*
194 *Phys.*, 5, 348.

195 Batista, I. S., R. T. Medeiros, M. A. Abdu, J. R. deSouza, G. J. Bailey, and E. R. dePaula
196 (1996), Equatorial ionospheric vertical plasma drift model for the Brazilian region, *J.*
197 *Geophys. Res.*, 101, 10,887–92.

198 De Boor, C. (2001), *A Practical Guide to Splines*, Springer, New York.

199 Draper, N., and H. Smith (1981), *Applied Regression Analysis, Second Edition*, John
200 Wiley & Sons, Inc, New York.

201 Fejer, B. G., E. R. de Paula, R. A. Heelis, and W. B. Hanson (1995), Global equatorial
202 ionospheric vertical plasma drifts measured by the AE-E satellite, *J. Geophys. Res.*,
203 100(A4).

204 Fejer, B. G., J. W. Jensen, and S.-Y. Su (2008), Quiet-time equatorial *F* region verti-
205 cal plasma drift model derived from ROCSAT-1 observations, *J. Geophys. Res.*, 113,
206 A05304, doi:10.1029/2007JA012801.

207 Forbes, J. M. (1981), The equatorial electrojet, *Reviews of Geophysics and Space Physics*,
208 19(3), 469–504.

209 Heelis, R. A. (2004), Electrodynamics in the low and middle latitude ionosphere: a tuto-
210 rial, *J. Atmos. Sol. Terres. Phys.*, 66, 825–38.

211 Kudeki, E., and C. D. Fawcett (1993), High resolution observations of 150 km echoes at
212 Jicamarca, *Geophys. Res. Lett.*, 18.

213 Pingree, J. E., and B. G. Fejer (1987), On the height variation of the equatorial *F* region
214 vertical plasma drift, *J. Geophys. Res.*, 92(A5), 4763–66.

215 Richards, P. G., J. A. Fennelly, and D. G. Torr (1994), EUVAC: A solar EUV flux model
216 for aeronomic calculations, *J. Geophys. Res.*, *99*(A5).

217 Sastri, J. H. (1996), Longitudinal dependence of equatorial F region vertical plasma drifts
218 in the dusk sector, *J. Geophys. Res.*, *101*(A2), 2445–52.

219 Scherliess, L., and B. G. Fejer (1999), Radar and satellite global equatorial F region
220 vertical drift model, *J. Geophys. Res.*, *104*(A4), 6829–42.

221 Su, Y. Z., K.-I. Oyama, G. J. Bailey, T. Takahashi, and S. Watanabe (1995), Comparison
222 of satellite electron density and temperature measurements at low latitudes with a
223 plasmasphere-ionosphere model, *J. Geophys. Res.*, *100*, 14,591–605.

224 Wessel, P., and W. H. F. Smith (1991), Free software helps map and display data, *EOS*
225 *Trans. AGU*, *72*(41), 441.

226 Woodman, R. F., and F. Villanueva (1995), Comparison of electric fields measured at F
227 region heights with 150 km irregularity drift measurements, *Proceedings of the Ninth*
228 *International Symposium on Equatorial Aeronomy, Bali, Indonesia.*

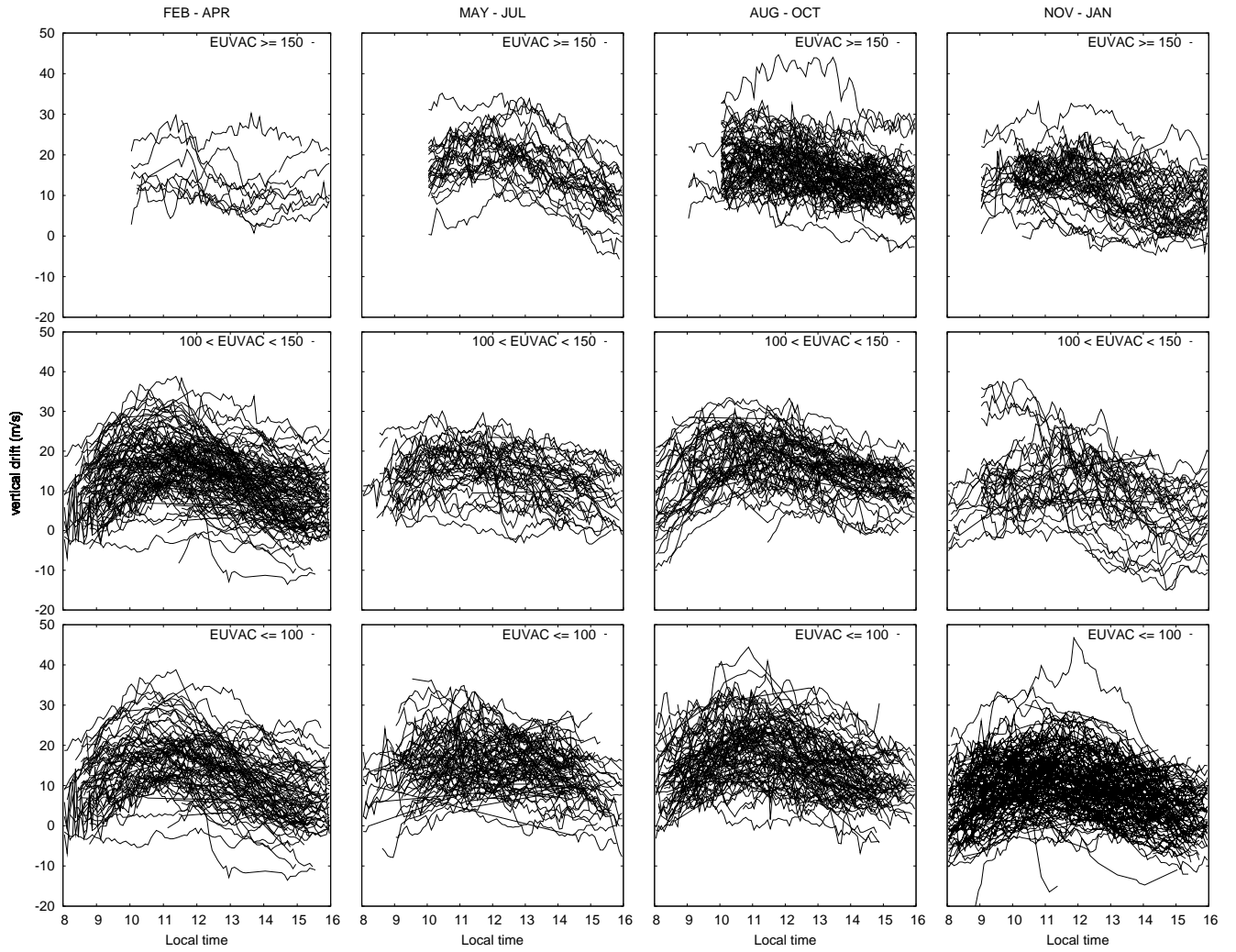


Figure 1. Local time profiles of JULIA quiet-time ($K_p \leq 3$) vertical drifts for low, medium and high solar activity and different seasons.

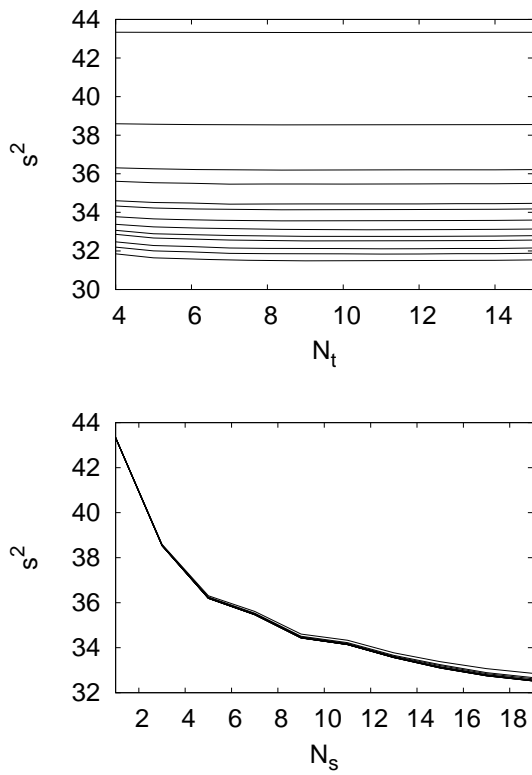


Figure 2. Residual mean square as a function of number of basis functions for each parameter of local time and season.

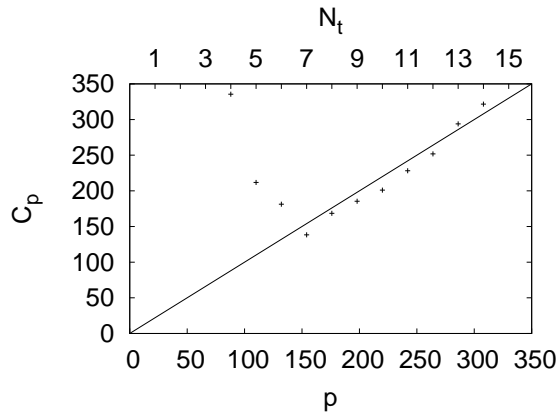


Figure 3. Mallows C_p statistic as a function of the total number of model parameters p , along with the line $C_p = p$.

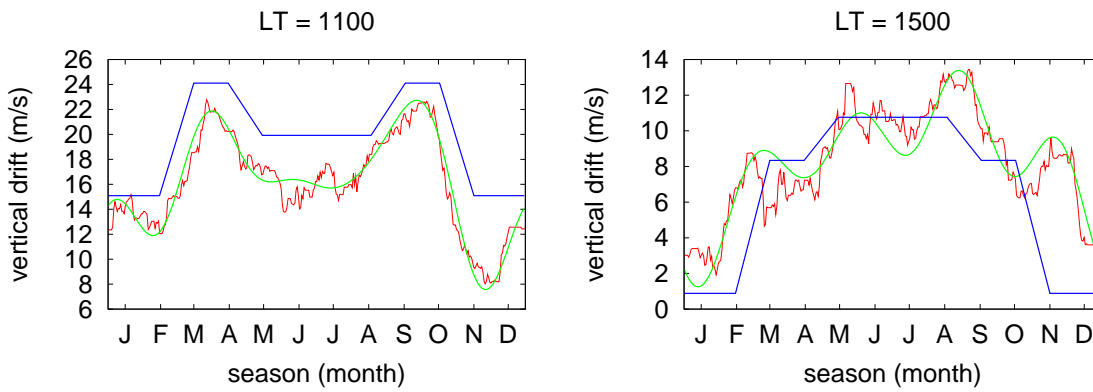


Figure 4. Comparison of Scherliess/Fejer model output (blue), JVDM model output (green) and raw JULIA data smoothed with a moving average of 30 days (red) as a function of season. An EUVAC index of 80 was used for the model outputs and the JULIA data was selected for EUVAC < 100 and with a local time window of $\pm 1/2$ hour around 1100 (left) and 1500 (right) local times.

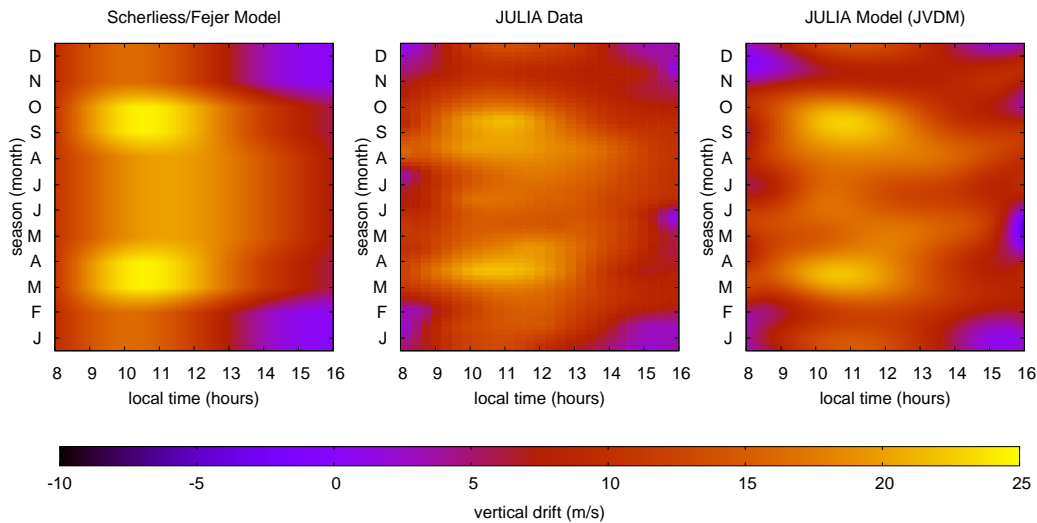


Figure 5. Scherliess and Fejer model output (left), raw JULIA vertical drift data (middle) and JULIA Vertical Drift Model output using EUVAC index of 80 (right).

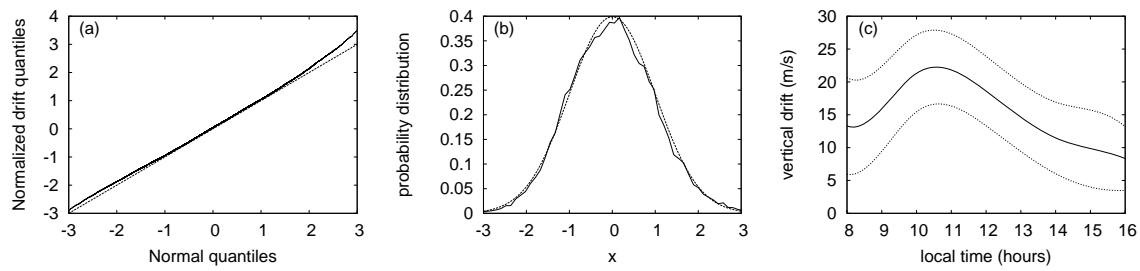


Figure 6. (a) Quantile-quantile plot with normalized drift quantiles vs normal quantiles. (b) Probability density function of normalized drift data along with ideal normal density profile. (c) Vertical drift local time profile (solid) with \pm standard deviation curves (dashed) for March equinox and EUVAC index of 100.